International Journal of Radiation Oncology biology • physics

www.redjournal.org

Clinical Investigation

Study of 201 Non-Small Cell Lung Cancer Patients Given Stereotactic Ablative Radiation Therapy Shows Local Control Dependence on Dose Calculation Algorithm

Kujtim Latifi, PhD,* Jasmine Oliver, BS,*,† Ryan Baker, BS,‡ Thomas J. Dilling, MD,* Craig W. Stevens, MD, PhD,* Jongphil Kim, PhD,§ Binglin Yue, MS,§ MaryLou DeMarco, MS, CMD,* Geoffrey G. Zhang, PhD,* Eduardo G. Moros, PhD,* and Vladimir Feygelman, PhD*

**Department of Radiation Oncology, Moffitt Cancer Center, †Department of Physics, University of South Florida, ‡University of South Florida School of Medicine, and §Department of Biostatics and Bioinformatics, Moffitt Cancer Center, Tampa, Florida*

Received Aug 16, 2013, and in revised form Dec 7, 2013. Accepted for publication Dec 27, 2013.

Summary

This study demonstrates the dependence of local control on the dose calculation algorithms used for treatment planning for non-small cell lung cancer patients treated with stereotactic ablative radiation therapy.

Purpose: Pencil beam (PB) and collapsed cone convolution (CCC) dose calculation algorithms differ significantly when used in the thorax. However, such differences have seldom been previously directly correlated with outcomes of lung stereotactic ablative body radiation (SABR).
Methods and Materials: Data for 201 non-small cell lung cancer patients treated with SABR were analyzed retrospectively. All patients were treated with 50 Gy in 5 fractions of 10 Gy each. The radiation prescription mandated that 95% of the planning target volume (PTV) receive the prescribed dose. One hundred sixteen patients were planned with BrainLab treatment planning software (TPS) with the PB algorithm and treated on a Novalis unit. The other 85 were planned on the Pinnacle TPS with the CCC algorithm and treated on a Varian linac. Treatment planning objectives were numerically identical for both groups. The median follow-up times were 24 and 17 months for the PB and CCC groups, respectively. The primary endpoint was local/marginal control of the irradiated lesion. Gray's competing risk method was used to determine the statistical differences in local/marginal control rates between the PB and CCC groups.
Results: Twenty-five patients planned with PB and 4 patients planned with the CCC algorithms to the same nominal doses experienced local recurrence. There was a statistically significant difference in recurrence rates between the PB and CCC groups (hazard ratio 3.4 [95% confidence interval: 1.18-9.83], Gray's test $P = .019$). The differences (Δ) between the 2 algorithms for target coverage were as follows: $\Delta D99_{GITV} = 7.4$ Gy, $\Delta D99_{PTV} = 10.4$ Gy, $\Delta V90_{GITV} = 13.7\%$, $\Delta V90_{PTV} = 37.6\%$, $\Delta D95_{PTV} = 9.8$ Gy, and $\Delta D_{ISO} = 3.4$ Gy. GITV = gross internal tumor volume.
Conclusions: Local control in patients receiving who were planned to the same nominal dose with PB and CCC algorithms were statistically significantly different. Possible alternative explanations are described in the report, although they are not thought likely to explain the difference. We

Reprint requests to: Kujtim Latifi, PhD, Moffitt Cancer Center, 12902 Magnolia Dr/MCC-Rad Onc, Tampa, FL 33612; Tel: (813) 745-1291; E-mail: Kujtim.Latifi@Moffitt.org

Conflict of interest: none.

Int J Radiation Oncol Biol Phys, Vol. ■, No. ■, pp. 1–6, 2014
0360-3016/$ - see front matter
http://dx.doi.org/10.1016/j.ijrobp.2013.12.047

conclude that the difference is due to relative dosimetric underdosing of tumors with the PB algorithm. © 2014 Elsevier Inc.

Introduction

The subject of heterogeneity corrections for dose calculation in the thoracic region has received much attention in the literature (1). In recent years, the importance of accurate dose calculations in the lung has only grown, because stereotactic ablative body radiation (SABR) has evolved to become a standard modality for definitively treating inoperable non-small cell lung cancer (NSCLC) patients, with reported local control rates up to 100% for stage I disease (2). Dose calculation algorithms that take into account lateral electron transport in inhomogeneous media are more accurate in the thoracic region, particularly at the periphery of small tumors in lung (3). Algorithms in the convolution/superposition family rely on precomputed kernels that are scaled with medium density and as such implicitly account for lateral scattering in small fields used for SABR. Although small systematic disagreement has been found between the practical convolution/superposition calculations and Monte Carlo simulations, which are considered the gold standard (4), for the purposes of this work, the collapsed cone convolution (CCC) algorithm implemented in the Pinnacle treatment planning system (Philips Radiation Oncology Systems, Fitchburg, WI) can be considered to provide a reasonable estimate of the actually delivered dose (5). Although the limitations of algorithms with 1-dimensional density scaling, such as pencil beam (PB), are known (1, 3), and they are not allowed in current Radiation Therapy Oncology Group lung SABR trials, a popular radiosurgery system originally relying on a PB algorithm (Novalis with Exac Trac and iPlan TPS, Brainlab AG, Feldkirchen, Germany) has been rather widely used in SABR treatment (6-12). The PB algorithm, when used with heterogeneity correction, overestimates dose to the planning target volume (PTV) by up to 40% (7, 13, 14). Consequently, when the monitor units are set based on the PB calculations, the actual delivered dose is proportionately lower than the prescription.

It is assumed that there should be a dose−response relationship in lung SABR (15). Some studies suggest an improved local control with a biologically equivalent dose (BED) $\geq$100 Gy (15, 16). One way to elucidate such a relationship is by directly comparing the outcomes of SABR treatments planned with the PB versus convolution/superposition or Monte Carlo type algorithms. However, such a task is confounded by multiple variables in the studies reported in the literature, such as variances in prescription dose and fractionation (17).

At our institution we have a large cohort of NSCLC patients treated with SABR to the lung (n=201), with reasonably long follow-up times (median, 23 months) treated by the same 2 physicians using the same target definition, prescription, and fractionation. Approximately 60% of the patients (n=116) were planned using PB, and the remainder (n=85) using CCC calculations. We hypothesized that local recurrence rates would be higher for the patients planned with the PB algorithm. We present here our findings.

Methods and Materials

Data for our first 201 NSCLC patients, treated with SABR from September 2006 to March 2011, were available for this study and were analyzed retrospectively with approval by our institutional review board (IRB #105996). All patients were treated to the same nominal prescription dose of 50 Gy in 5 fractions of 10 Gy each. The radiation prescription mandated that 95% of the PTV received the prescribed dose of 50 Gy. One hundred percent of the gross internal tumor volume (GITV) was mandated to receive the prescribed dose. No specific ratio of the PTV peripheral to maximum dose was enforced. However, the near-minimum PTV dose (D_{99}) was higher than 90% of prescription. Patients with tumor histologies other than NSCLC, or different dose fractionation schemas, were excluded from the analysis. Initially, all patients were planned with a PB algorithm and treated on the Novalis unit. Subsequently, linacs with cone beam computed tomography (CBCT) became available in our department. At that point, we discontinued lung SABR treatment on the Novalis unit. All patients were treated from Monday to Friday on 5 consecutive days.

Simulation of all patients was done by use of a helical 4-dimensional (4D) CT scan on Philips Brilliance CT (Philips Medical Systems, Cleveland, OH), with the respiratory phase trace provided by the bellows. The GITV was derived from (at a minimum) the union of the GTV volumes on 2 extreme phases of the respiratory scan and the free-breathing scan. No GTV-to-CTV margin was added. The standard GITV-to-PTV expansion was 5 mm axially and 7 mm superiorly and inferiorly. Dose calculations were performed on the slow (low-pitch) untagged scan.

All patients were immobilized for treatment with a BodyFix double-vacuum cradle (Elekta AB, Stockholm, Sweden). To minimize respiratory excursion of the diaphragm, patients typically underwent abdominal compression. Some patients did not undergo any abdominal compression, either because of poor tolerance or because a CT simulation without abdominal compression demonstrated minimal respiratory motion of the tumor.

The first 116 patients were planned by use of a heterogeneity-corrected PB algorithm (BrainLab iPlan, version 3.02). A 3-dimensional (3D) conformal technique with 5 to 7 noncoplanar beams was used. Treatments were delivered on a 6-MV Novalis linear accelerator with an integrated micro-multileaf collimator with 3-mm leaves (BrainLab). Daily image guidance was performed with stereoscopic imaging (Novalis ExacTrac). All patients had fiducials implanted into or near the tumor. Those fiducials were contoured on all phases of the 4D CT scan, and the unions of those respective contours (fiducial ITVs) were overlaid on the alignment digitally reconstructed radiographs. Before each treatment, the bony anatomy alignment was peformed first. Then the treating physician verified that the fiducials on the localization radiographs were situated within their respective mini-ITVs on the alignment digitally reconstructed radiographs, and additional shifts were performed if necessary. Given that prolonged treatment time is associated with increased probability of a systematic intrafraction shift (18), patients underwent reimaging (and shifts, if appropriate) after half the beams were delivered, and at additional time points, at the direction of the treating physician. In an early study of our first 29 SABR patients, we found that the mean midtreatment shifts were 2.4, 3.1, and 2.0 mm in the lateral, longitudinal, and vertical directions, respectively (19).

Table 1 Baseline patient characteristics

Characteristic	PB, n (%)	CCC, n (%)	*P* value
Sex			
M	61 (52.6)	44 (51.8)	1.0000*
F	55 (47.4)	41 (48.2)	
Age (y)			
Median (range)	73.0 (37.0-93.0)	72.0 (49.0-89.0)	.2706†
Physician 1	55 (47)	43 (50)	.6709*
Physician 2	61 (53)	42 (50)	
Histology			
Adenocarcinoma	60 (51.2)	44 (51.7)	.4379*
Squamous cell	23 (19.8)	21 (24.7)	
Neuroendocrine	1 (0.9)	1 (1.2)	
Mixed histology	5 (4.3)	1 (1.2)	
Large cell	0	1 (1.2)	
Sarcomatoid	1 (0.9)	1 (1.2)	
NSCLC (NOS)	24 (20.5)	13 (15.2)	
Presumptive‡	2 (1.7)	3 (3.5)	
Tumor classification			
T1§	103 (88.8)	61 (71.8)	.0035*
T2§	13 (11.2)	23 (27.1)	
T3§	0 (0.0)	1 (1.2)	
Charlson Comorbidity Index (age-adjusted)			
Median	6.0 (0.0, 13.0)	6.0 (0.0, 13.0)	.6436†
Treatment lobe			
RUL	35 (30.2)	24 (28.2)	.2451*
RLL	26 (22.4)	31 (36.5)	
RML	8 (6.9)	5 (5.9)	
LUL	27 (23.3)	16 (18.8)	
LLL	20 (17.2)	9 (10.6)	

Abbreviations: LLL = left lower lobe; LUL = left upper lobe; NOS = not otherwise specified; NSCLC = non-small cell lung cancer; RLL = right lower lobe; RML = right middle lobe; RUL = right upper lobe.

* Fisher test.

† Wilcoxon test.

‡ A small number of lesions did not undergo biopsy (n=5) in patients with pre-existing locally advanced NSCLC with metachronous lesion radiographically suspected of being metastasis from the prior cancer.

§ Patients were initially staged according to the staging system in use at the time of their presentation to our institution. For purposes of this study, all patients were retrospectively restaged by use of the American Joint Committee on Cancer, seventh edition.

The subsequent 85 patients were planned with a heterogeneity-corrected CCC algorithm. Either 3D conformal or volumetric arc therapy (VMAT) techniques were used, with beam energies ranging from 6 to 15 MV. The 3D conformal beam arrangements were similar to the PB plans, whereas the VMAT treatments consisted of 2 or (rarely) 3 hemiarcs avoiding beam entrance through the contralateral lung. Those patients were treated on either a Trilogy or a TrueBeam machine (Varian Medical Systems, Palo Alto, CA) equipped with a 120-leaf Millennium multileaf collimator (5-mm leaves in the central portion of the field). Daily image guidance was provided by CBCT, with alignment to the visible tumor on the untagged planning scan. Dose voxel size was kept at 2 mm for both algorithms.

The median follow-up times were 24 and 17 months for the PB and CCC groups, respectively, calculated from the last day of treatment. The primary endpoint was local/marginal control of the irradiated lesion. Workup of treatment failure varied, depending on the patients' clinical situation. Patients were routinely followed up with CT scans every 3 months for the first 2 years, every 4 months for a year, every 6 months for 2 more years, then yearly after 5 years. The recurrent lesions all demonstrated interval growth on these scans. When possible, biopsy confirmation was obtained, always at least 6 months after treatment, given the expected high rate of pathologic positivity otherwise. In some cases, lesions were not amenable to repeated biopsy. Positron emission tomography/CT was used to confirm recurrence no less than 6 months after treatment because of the confounding factor of treatment-related changes/inflammation. Typically, trial courses of antibiotics were used to rule out infection as a confounding factor. Local versus marginal failure was defined by the treating radiation oncologist. Marginal failures were immediately (<1 cm) outside the area of posttreatment consolidation. Local failures were defined as occurring within the area of posttreatment consolidation. In a few cases, however, the area of posttreatment lung change was drastically larger than the lesion originally treated. In these few cases, recurrences in the periphery of the region of pneumonitis/fibrosis were defined as marginal.

Statistical analysis was performed with SAS, version 9.2, software (SAS Institute Inc., Cary, NC). Accounting for competing risk events, the difference between the 2 groups was assessed by Gray's method (20). A 2-sided *P* value of <.05 was considered statistically significant. Potential influence of age, sex, T stage, or treating physician on the recurrence rate was examined by univariable models. To eliminate the possibility of a learning curve negatively influencing the outcomes, we repeated the analysis temporarily excluding patients (n=32) treated during the first year of the program. This also provided additional insight into whether the observed local control differences could be due to the different follow-up lengths for the PB and CCC cohorts, by eliminating the study participants with potentially longest follow-up times.

Forty-nine plans calculated with PB (24 with and 25 without local recurrence) were recalculated with the CCC algorithm, without changing any beam parameters. By doing so we were able to estimate the average difference between the calculated PB dose and the approximation of the delivered dose. Near minimum dose (D_{99} [PTV, GITV]), minimum dose to 95% of the volume (D_{95PTV}), volume receiving 90% of prescription (V_{90} [PTV, GITV]), and the isocenter dose (D_{ISO}) were chosen as representative dosimetric indices for comparison.

Results

Patients' characteristics were generally well balanced between the 2 groups (Table 1). There was also a trend for the patients planned with PB to have smaller (T1a-T1b) lesions than those in the CCC group. Twenty-five patients (21.5% crude rate) planned with PB and 4 patients (4.7%) planned with the CCC algorithms experienced local recurrence. There was a significant difference in recurrence rates between the PB and CCC groups (Fig. 1) (hazard ratio [HR] = 3.4; 95% confidence interval [CI]: 1.18-9.83, Gray's test *P*=.019). Age, sex, physician, and T stage were not associated with the rate of recurrence.

Of note, the PB group had statistically smaller cancers (Table 1) and yet showed statistically diminished local control compared with the CCC cohort.

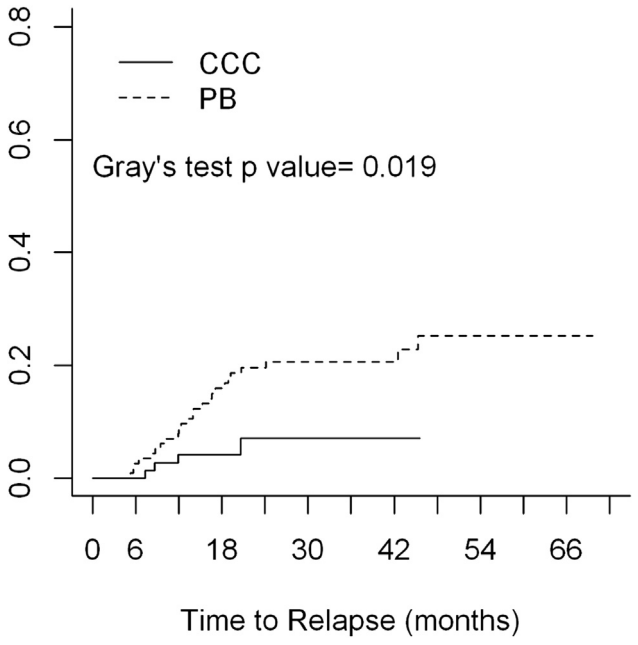

Fig. 1. Cumulative incidence of recurrence by group for all patients (N=201): pencil beam (PB) versus collapsed cone convolution (CCC).

With the first 32 (PB) patients eliminated from analysis, there is equally statistically significant difference in recurrence rates between the PB and CC groups (Fig. 2). Hazard ratio is 3.7 (95% CI: 1.25-10.93), Gray's test $P=.013$. Again, age, sex, physician, and T stage were not prognostic factors.

Table 2 shows the mean differences of dose metrics between the same plans computed with PB and CCC for 24 patients with locally recurring disease and 25 randomly chosen patients with nonrecurring disease. The average differences (Δ) between the 2 algorithms (n=49) for target coverage in otherwise identical plans were as follows: $\Delta D99_{GITV} = 7.4$ Gy, $\Delta D99_{PTV} = 10.4$ Gy, $\Delta V90_{GITV} = 13.7\%$, $\Delta V90_{PTV} = 37.6\%$, $\Delta D95_{PTV} = 9.8$ Gy, and $\Delta D_{ISO} = 3.4$ Gy. The differences between the 2 groups are statistically insignificant. The reduction in PTV D95 was additionally analyzed in terms of edge versus island tumors as defined by Zhuang et al (21). There was a statistically significant difference (*t* test $P=.023$) between 13 island and 36 edge tumors. The average drop in PTV D95 was 22.9 ± 6.8% (1 SD) and 17.4 ± 7.4% for island and edge tumors, respectively. These averages agree reasonably well with the published PB versus Monte Carlo data (23.8/15.3%) (21). There were no statistically significant differences in PTV D95 reduction for island and edge subgroups between the patients with recurring disease and those without.

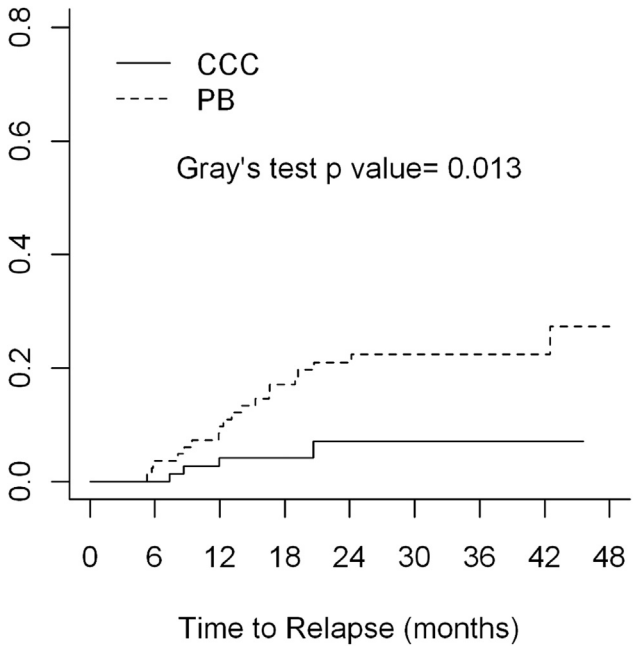

Fig. 2. After removal of 32 pencil beam (PB) patients treated during the first year of our stereotactic ablative body radiation program, the difference in outcome between PB and collapsed cone convolution (CCC) remained statistically significant.

Table 2 Differences of dose–volume metrics for the same plans calculated with PB and CCC algorithms, for 24 failures and 25 randomly chosen nonfailures. There were no statistically significant differences between the means of the failures and nonfailures, $P=.53$ to .98

	Failures				Nonfailures			
Dose–volume	Mean	Max	Min	SD	Mean	Max	Min	SD
D99 (GITV)	7.3	14.7	1.7	3.3	8.2	13.7	2.5	3.3
V90 (GITV)	15.0	74.7	0.0	23.6	12.4	56.5	0.0	15.8
D99 (PTV)	10.6	19.2	0.7	5.1	11.3	20.1	1.2	4.8
D95 (PTV)	10.0	18.2	0.3	4.6	10.6	17.9	2.9	3.8
V90 (PTV)	36.3	97.7	0.4	31.5	38.9	85.1	4.3	23.0
D_{ISO}	3.3	5.9	1.1	1.3	3.7	8.1	1.2	1.7

Abbreviations: CCC = collapsed cone convolution; D95 = minimum dose to 95% of volume; D99 = near-minimum PTV dose; D_{ISO} = isocenter dose; GITV = gross internal tumor volume; Max = maximum; Min = minimum; PTV = planning target volume; SD = standard deviation.

Discussion

We found a statistically significant difference in local control between patients planned to the same nominal prescription 50-Gy dose with the PB and CCC algorithms. Although there was a 78% crude local control rate in patients planned with PB, the local control rate for patients planned with CCC was 95%. Because the delivered (D95) dose to the PTV was, on average, 18.6% lower for the PB cohort (see representative example in Fig. 3), it appears that a dose–response relationship has been empirically confirmed. Prior studies have suggested that a minimum BED of 100 Gy is necessary for improved outcome with SABR (15, 16). Certainly, others have questioned the applicability of the linear quadratic model (and therefore BED calculations) at very high fractional radiation therapy doses (22). Whether or not BED estimates are justified, our results are consistent with those prior publications. Overall, our PB local control data are within the range presented in the recent systematic review by Solda et al (2), albeit below the average for stage I disease (78% vs weighted mean of 91% with 95% CI of 90%-93%). Our PB patients were treated very similarly to those of Videtic et al (23) in terms of prescription, calculation algorithm, and treatment equipment. The lower local control rate

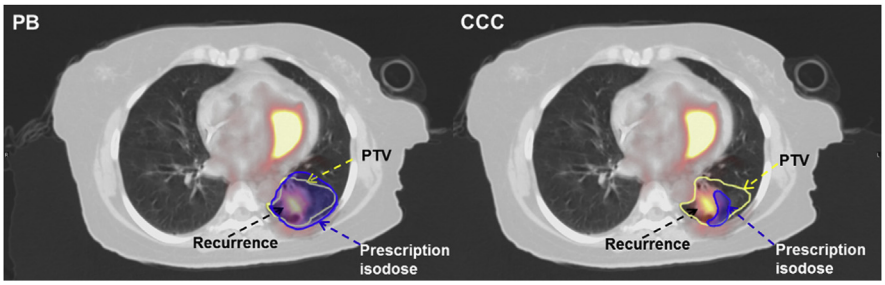

Fig. 3. Example of pencil beam (PB) algorithm dose overestimation compared with collapsed cone convolution (CCC) algorithm in a patient receiving 50 Gy in 5 fractions. Positron emission tomography recurrence image is overlaid with the planning computed tomographic image showing the planning target volume (PTV) and prescription isodose for both treatment planning systems. (A) PB treatment plan reflecting PTV D95 of 50 Gy. (B) CCC recalculation shows underdosage: PTV D95 = 43 Gy.

(78 vs >93%) does not have a definitive explanation in that context. It is, however, consistent with the idea that a dose regimen of 50 Gy in 5 fractions to 95% of the PTV is right at the cusp of the BED adequate for local control. Such a regimen may not be robust enough with respect to uncontrolled local variations in planning and/or treatment execution, resulting in widely varying control rates. This reasoning is in agreement with the data from a study by Olsen et al (16). In that work, reducing the prescription from 10 Gy in 5 fractions to 9 Gy in 5 fractions, with convolution-superposition (ie, realistic) dose calculations and CBCT guidance, was the only significant prognostic factor in reduction of the 1-year crude local control from 99%-100% to 75%. The 9-Gy convolution dose is comparable to, or higher than, our 10-Gy PB dose, resulting in a similar control rate. On the other hand, Baumann et al (6), using a heterogeneity-corrected PB algorithm, reported a 100% local control rate for T1 tumors for a more biologically effective fractionation scheme of 45 Gy in 3 treatments. This more aggressive prescription may be more forgiving in terms of delivered dose being lower than nominal.

This retrospective review has its limitations. An important one is the difference in follow-up times between the PB and CCC cohorts. This is a result of the retrospective study design based on technology change midstream. The real question is whether the follow-up time in the later cohort was long enough to enable most failures to be observed. In this study, the median follow-up time of the shorter of the 2 cohorts (17 months) was longer than the overall median follow-up times in other studies asking similar questions (15-17), particularly for the Monte Carlo group in the study by Liu et al (17). As indicated in Figure 1, the recurrence curves start to diverge before 6 months, and they substantially flatten out after 17 months, the median follow-up time of the later (CCC) cohort. The exclusion of 8 PB patients who experienced recurrence more than 17 months after treatment did not negate statistical significance in difference between the cohorts (data not shown).

Another potential bias that this study cannot quantitatively address is the difference in image guidance techniques between the 2 cohorts, namely stereoscopic radiographs versus CBCT. Both systems are capable of localizing a hidden target in a rigid phantom with submillimeter accuracy (24, 25). In vivo, there is a risk with the planar images of a gross geographic miss in lung resulting from the alignment to an incorrect vertebral body. However, the use of fiducial markers, as opposed to just bony anatomic landmarks, should mitigate this risk. Corradetti et al (26) concluded that stereoscopic alignment to bone anatomy is suboptimal for lung SABR. However, in our case, by keeping the fiducials within their mini-ITVs on the radiographs, we essentially were aligning to the tumor surrogate rather than just to the bony anatomy. Even with this approach, CBCT has an advantage in that it inherently averages the tumor location during the respiratory cycle, whereas planar images are just snapshots in time. In the context of this study, it is impossible to quantify the improvement in accuracy afforded by aligning to the fiducials, but one can reasonably assume that there is some. In particular, the systematic standard deviation Σ, key to margin estimates (27), should be reduced. Alignment to the fiducials would likely have the effect of substantially reducing the largest offsets between kV and CBCT localization, such as a 14.6-mm discrepancy showcased in the study by Shah et al (28) for a patient with scoliosis. These largest discrepancies are those driving up the standard deviation Σ. Even with alignment to the bone anatomy, the difference between kV and CBCT methods is similar in magnitude to the intrafraction motion (26, 28), and as of 2010, both methods were used in the United States for IGRT in approximately equal proportions (29). Fiducial positioning in lung is sufficiently stable (30). Although CBCT localization may be theoretically advantageous (26), to the best of our knowledge, there are no published data clearly demonstrating superior clinical outcomes in lung SABR using CBCT for image guidance, as compared with stereoscopic radiographs.

There were also differences in the patient cohorts in terms of treatment techniques (3D vs VMAT) and beam energies (10 or 15 MV was used on some CCC patients, whereas the PB patients had only 6 MV available). Although inversely planned techniques such as VMAT may produce better results in terms of dose conformality and healthy tissue sparing (31, 32), the important parameter in the context of this study is tumor coverage, where both techniques are forced to the same dosimetric result. The effect of motion interplay on the tumor dose−volume histogram in VMAT lung SABR is negligible (33). Because 10- to 15-MV beams were used only with the CCC algorithm, the lateral dose spread in lung, characteristic of higher energies, was handled with reasonable dosimetric accuracy. In general, a systematic review by Solda et al (2) indicated no difference in outcome results for stage I NSCLC in terms of broadly grouped delivery technology options.

Conclusions

A single-institution retrospective study of 201 patients treated with SABR for NSCLC showed that local/marginal control was statistically significantly improved for the 50 Gy in 5 fractions

prescription when dose calculation was performed by use of the CCC algorithm compared with PB. With the same nominal prescription, CCC consistently resulted in higher delivered dose than with PB: 18.6% on average for the PTV D95. Because the nominal prescription dose had a BED of 100 Gy, which others have previously argued to be a minimum necessary for adequate local control (21, 22), it is consistent with those estimates that patients treated with nominal 50 Gy in 5 fractions by the use of PB-based heterogeneity corrected plans would have diminished local control.

References

1. Papanikolaou N, Battista JJ, Boyer AL, et al. *Tissue inhomogeneity corrections for megavoltage photon beams: Report of task group no. 65 of the radiation therapy committee: AAPM report no. 85*. Madison: Medical Physics Publishing; 2004.
2. Solda F, Lodge M, Ashley S, et al. Stereotactic radiotherapy (SABR) for the treatment of primary non-small cell lung cancer: Systematic review and comparison with a surgical cohort. *Radiother Oncol* 2013; 109:1-7.
3. Benedict SH, Yenice KM, Followill D, et al. Stereotactic body radiation therapy: The report of AAPM task group 101. *Med Phys* 2010; 37:4078-4101. Erratum in: Med Phys 2012;39:563. Dosage error in article text.
4. Kry SF, Alvarez P, Molineu A, et al. Algorithms used in heterogeneous dose calculations show systematic differences as measured with the radiological physics center's anthropomorphic thorax phantom used for RTOG credentialing. *Int J Radiat Oncol Biol Phys* 2013;85:e95-e100.
5. Krieger T, Sauer OA. Monte carlo- versus pencil-beam-/collapsed-cone-dose calculation in a heterogeneous multi-layer phantom. *Phys Med Biol* 2005;50:859-868.
6. Baumann P, Nyman J, Hoyer M, et al. Outcome in a prospective phase II trial of medically inoperable stage I non-small-cell lung cancer patients treated with stereotactic body radiotherapy. *J Clin Oncol* 2009;27:3290-3296.
7. Ding GX, Duggan DM, Lu B, et al. Impact of inhomogeneity corrections on dose coverage in the treatment of lung cancer using stereotactic body radiation therapy. *Med Phys* 2007;34:2985-2994.
8. Fakiris AJ, McGarry RC, Yiannoutsos CT, et al. Stereotactic body radiation therapy for early-stage non−small-cell lung carcinoma: Four-year results of a prospective phase II study. *Int J Radiat Oncol Biol Phys* 2009;75:677-682.
9. Haasbeek CJ, Lagerwaard FJ, Antonisse ME, et al. Stage I nonsmall cell lung cancer in patients aged $>$ or $=$75 years: Outcomes after stereotactic radiotherapy. *Cancer* 2010;116:406-414.
10. Mehta N, King CR, Agazaryan N, et al. Stereotactic body radiation therapy and 3-dimensional conformal radiotherapy for stage I non-small cell lung cancer: A pooled analysis of biological equivalent dose and local control. *Pract Radiat Oncol* 2012;2:288-295.
11. Rubio MC, Hernando O, Sánchez E, et al. Clinical experience on the treatment of lung and liver lesions with stereotactic body radiotherapy using a novalis exactrac adaptive gating technique. *Clin Oncol* 2011; 23:S16.
12. Timmerman R, Paulus R, Galvin J, et al. Stereotactic body radiation therapy for inoperable early stage lung cancer. *JAMA* 2010;303:1070-1076.
13. Lax I, Panettieri V, Wennberg B, et al. Dose distributions in SBRT of lung tumors: Comparison between two different treatment planning algorithms and Monte-Carlo simulation including breathing motions. *Acta Oncol* 2006;45:978-988.
14. Taylor ML, Kron T, Franich RD. A contemporary review of stereotactic radiotherapy: Inherent dosimetric complexities and the potential for detriment. *Acta Oncol* 2011;50:483-508.
15. Guckenberger M, Wulf J, Mueller G, et al. Dose-response relationship for image-guided stereotactic body radiotherapy of pulmonary tumors: Relevance of 4D dose calculation. *Int J Radiat Oncol Biol Phys* 2009; 74:47-54.
16. Olsen JR, Robinson CG, El Naqa I, et al. Dose-response for stereotactic body radiotherapy in early-stage non-small-cell lung cancer. *Int J Radiat Oncol Biol Phys* 2011;81:E299-E303.
17. Liu MB, Eclov NCW, Trakul N, et al. Clinical impact of dose overestimation by effective path length calculation in stereotactic ablative radiation therapy of lung tumors. *Pract Radiat Oncol* 2013;3:294-300.
18. Purdie TG, Bissonnette JP, Franks K, et al. Cone-beam computed tomography for on-line image guidance of lung stereotactic radiotherapy: Localization, verification, and intrafraction tumor position. *Int J Radiat Oncol Biol Phys* 2007;68:243-252.
19. Dilling TJ, Chuong M, Sarangkasiri S, et al. Evaluation of patient setup variability between two different immobilization systems used for SBRT or standard fractionation IGRT in the treatment of lung cancers on a Novalis treatment unit. *Int J Radiat Oncol Biol Phys* 2007;69 (Suppl):S514.
20. Gray R. A class of k-sample tests for comparing the cumulative incidence of a competing risk. *Ann Statistics* 1988;16:1141-1154.
21. Zhuang T, Djemil T, Qi P, et al. Dose calculation differences between Monte Carlo and pencil beam depend on the tumor locations and volumes for lung stereotactic body radiation therapy. *J Appl Clin Med Phys* 2013;14:38-51.
22. Fowler JF. The linear-quadratic formula and progress in fractionated radiotherapy. *Br J Radiol* 1989;62:679-694.
23. Videtic GM, Stephans K, Reddy C, et al. Intensity-modulated radiotherapy-based stereotactic body radiotherapy for medically inoperable early-stage lung cancer: Excellent local control. *Int J Radiat Oncol Biol Phys* 2010;77:344-349.
24. Yan H, Yin FF, Kim JH. A phantom study on the positioning accuracy of the Novalis body system. *Med Phys* 2003;30:3052-3060.
25. Yan H, Zhang L, Yin F. A phantom study on target localization accuracy using cone-beam computed tomography. *Clin Med Oncol* 2008;2:501-510.
26. Corradetti MN, Mitra N, Bonner Millar LP, et al. A moving target: Image guidance for stereotactic body radiation therapy for early-stage non-small cell lung cancer. *Pract Radiat Oncol* 2013;3:307-315.
27. van Herk M, Remeijer P, Rasch C, et al. The probability of correct target dosage: Dose-population histograms for deriving treatment margins in radiotherapy. *Int J Radiat Oncol Biol Phys* 2000;47:1121-1135.
28. Shah C, Kestin LL, Hope AJ, et al. Required target margins for image-guided lung SBRT: Assessment of target position intrafraction and correction residuals. *Pract Radiat Oncol* 2013;3:67-73.
29. Simpson DR, Lawson JD, Nath SK, et al. A survey of image-guided radiation therapy use in the United States. *Cancer* 2010;116:3953-3960.
30. Imura M, Yamazaki K, Shirato H, et al. Insertion and fixation of fiducial markers for setup and tracking of lung tumors in radiotherapy. *Int J Radiat Oncol Biol Phys* 2005;63:1442-1447.
31. Merrow CE, Wang IZ, Podgorsak MB. A dosimetric evaluation of VMAT for the treatment of non-small cell lung cancer. *J Appl Clin Med Phys* 2012;14:228-238.
32. Holt A, van Vliet-Vroegindeweij C, Mans A, et al. Volumetric-modulated arc therapy for stereotactic body radiotherapy of lung tumors: A comparison with intensity-modulated radiotherapy techniques. *Int J Radiat Oncol Biol Phys* 2011;81:1560-1567.
33. Stambaugh C, Nelms BE, Dilling T, et al. Experimentally studied dynamic dose interplay does not meaningfully affect target dose in VMAT SBRT lung treatments. *Med Phys* 2013;40:091710.